Nig. J. Pure & Appl. Sci. Vol. 39 (Issue 1, 2026)
e-ISSN 2756-4045
(C) 2026 Faculty of Physical Sciences and Faculty of Life Sciences, Univ. of Ilorin, Nigeria
www.njpas.com.ng

Assesment of Percentage Depth Dose, Beam Flatness, and Beam Symmetry in Different Media of Different Photon Energy Beams using DOSXYZnrc Monte Carlo Code

*Olima, J. Omafu, Ibitoye, A. Z., Usen, I. and Ojo, B. E.

Department of Radiotion Biology, Radiotherapy and Radiodiagnosis, College of Medicine, University of Lagos, Idi-Araba, Lagos Nigeria

Date Received: 20-11-2025
Date Accepted: 28-01-2026
DOI: https://doi.org/10.48198/NJPAS/25.B44

ABSTRACT

In radiotherapy treatment planning, accurate dose calculation is important. Any difference in photon energy might affect dose deposition. The DOSXYZnrc Monte Carlo code was utilized to simulate photon interactions in heterogeneous media in order to evaluate dose distributions in water, lung, soft tissue, and bone. Photon energies of 6, 10, and 15 MV for sizes ranging from 5 × 5 to 20 × 20 cm² at a source-to-surface distance of 100 cm. Dose profile, percentage depth dose and beam uniformity parameters were analyzed to assess the effect of photon beam, field size and material density. The results obtained shows that higher photon energies improve beam penetration and reduce surface dose, while large field size increases scatter equilibrium and dose uniformity. Bone showed sharp dose fall-off and higher surface doses due to high density; on the other hand, lung showed deeper dose build-up and wide dose profiles across the energies and media. Beam flatness remains within ±3%, and symmetry within ±2%, consistent with clinical tolerance limits. The results indicate that DOSXYZnrc is a dependable and precise tool for enhancing treatment planning, dose validation, and photon beam simulation in radiotherapy. This work demonstrates the efficiency of Monte Carlo simulation in enhancing dose prediction accuracy across different tissues.

Keywords: *Radiotherapy, DOSXYZnrc, Monte Carlo, field size, photon energy, beam symmetry, beam flatness, percentage depth dose.*

Introduction

In cancer treatment, radiotherapy is considered one of the options for malignant tumours. The advancement of 3D techniques such as intensity-modulated radiotherapy (IMRT), image-guided radiotherapy (IGRT) and stereotactic radiation therapy has ensured delivery of accurate doses while minimizing exposure to surrounding healthy tissues (Baumann *et al.,* 201 6).

Intensity modulated radiation therapy (IMRT) delivers high dose distribution while sparing normal healthy tissues, but it comes with its own risks (Ayata et al., 2011; Sladowska *et al.*, 2011).

In heterogeneous media or complex geometries where conventional planning algorithms may be inadequate, a reliable dose calculation is important. Monte Carlo simulation is considered one of the most accurate approaches in addressing radiation transport in complex geometries. Although Monte Carlo software is considered time-consuming, it can reproduce physics interactions with high accuracy, which serves as a reliable tool for treatment verification (Bencheikh *et al.,* 2019).

Corresponding Author: **Olima J. Omafu**
Department of Radiotion Biology, Radiotherapy and Radiodiagnosis, College of Medicine, University of Lagos, Idi-Araba, Lagos Nigeria.
Email: olimajamesomafu@gmail.com Phone: +2349065080911

©2026 Creative Common License Attribution 4.0 International

This study utilized DOSXYZnrc Monte Carlo code to calculate absorbed dose, analyzing how different tissue compositions affect dose distribution (Machichi *et al.*, 2019). Photon energies of 6 MV, 10 MV, and 15 MV and different field sizes were analyzed across water, bone, lung, and soft tissue with the aim of improving the accuracy in radiotherapy treatment planning. A thorough understanding of these beam characteristics forms the basis for accurate dose calculation in heterogenous patient anatomies common in advanced techniques like IMRT.

2.0 Materials and Method

Monte Carlo simulations were carried out on EGSnrc using the DOSYZnrc code for modeling dose distribution. The simulations were carried out in Linux (Ubuntu 24.04.2 LTS) to ensure the compatibility with EGSnrc. The 700icru pegs4 data was utilized for all materials. dosxyz_show was used to visualized the generated output data. The dose profile and percentage depth dose were extracted from the simulation output and analyzed with Microsoft Excel.

For each simulation, DOSXYZnrc code was used, and the parameters were adjusted to obtain statistical results. Particle histories of 10 million up to 1 billion (NCASE = 1 x 10^7 to 1 x 10^9) were simulated to achieve a very high accuracy. The statistical uncertainty assessed along the central axis in the high-dose region was ~0.3% with a particle history of 1 x 10^9. A standard transport threshold was set as AE = 0.7 MeV and AP = 0.01 MeV. The electron energies and phantom energies were set at ECUT = 0.7 MeV and PCUT = 0.01 MeV.

The incident photon beam was simulated using a source type 0 parallel beam from the front. Spectrum photon energy of 6 MV, 10 MV, and 15 MV was used. Field sizes of 5 × 5 cm², 10 × 10 cm², 15 × 15 cm², and 20 × 20 cm² were set up at the phantom surface, and the phantom size was set at 30 × 30 × 30 cm^3 (x, y, z) for water, bone, soft tissue, and lung, and all simulations were carried out at an SSD of 100 cm.

The beam symmetry and beam flatness were computed using the following standard formulas by Podgorsak (2005).

Beam Flatness was defined as

$$F = 100 \times \frac{Dmax - Dmin}{Dmax + Dmin} \quad \text{(i)}$$

Where D_{max} and D_{min} are the maximum and minimum dose values within the central 80% of the beam width.

Beam symmetry S was determined at Z_{max} by comparing the areas under the lateral dose profile on either side of the central axis extending to the 50% dose level.

Symmetry was defined as

$$S = 100 \times \frac{arealeft - arearight}{arealeft + arearight} \quad \text{(ii)}$$

Where $area_{left}$ and $area_{right}$ are the integral dose areas on the left and right sides of the central axis respectively.

Table 1: Material Composition Used in Monte Carlo Simulations

Element	Z	Water	Soft Tissue	Lung	Bone
H	1	0.1119	0.1010	0.1030	0.0350
C	6		0.1190	0.1050	0.1550
O	8	0.8881	0.7650	0.7490	0.4100
N	7		0.0310	0.0310	0.0420
Ca	20				0.2250
P	15				0.1230
Z_{mean}			7.64	7.42	12.31
ρ(g/cm^3		0.998	1.00	0.26	1.85

3.0 Results

Phantoms of water, soft tissue, lung, and bone were generated using the DOSXYZnrc Monte Carlo code with photon energies of 6 MV, 10 MV and 15 MV and field sizes set at 5 × 5 cm², 10 × 10 cm², 15 × 15 cm², and 20 × 20 cm² at a source-to-surface distance of 100 cm.

The simulation generated a lateral dose profile and percentage depth dose (PDD) for each material used. All PDDs were extracted at a central beam axis to a depth of 30 cm and

lateral dose profile at D_{max}. Particle histories of 1×10^7 to 1×10^9 were run for all simulations, ensuring less uncertainty and high accuracy.

Across all materials, as the field size was increased from 5 × 5 cm² to 20 × 20 cm², it showed the impact of scattered radiation. Dose uniformity and percentage depth were produced by large field sizes.

From figures 4-6, lateral dose profiles were symmetrical and uniform for all energies and field sizes. The profile for soft tissue and water was flat with a small penumbra, whereas bone had a rapid dose fall-off. The dose profile for the lung was larger, showing an increase in lateral spread due to scatter equilibrium.

The standard clinical tolerance for beam flatness and symmetry is said to be within ±3% and ±2%. As presented in Table 2, the beam flatness and symmetry were within clinical tolerance. At 6 MV for a field size of 5 × 5 cm², the lung showed a large flatness variation of 0.755%, and soft tissue at 10 MV for a field size of 10 × 10 cm² had the least symmetry variation of 0.002%. Beam flatness increased with increasing field size, while symmetry remained constant for all energies and materials.

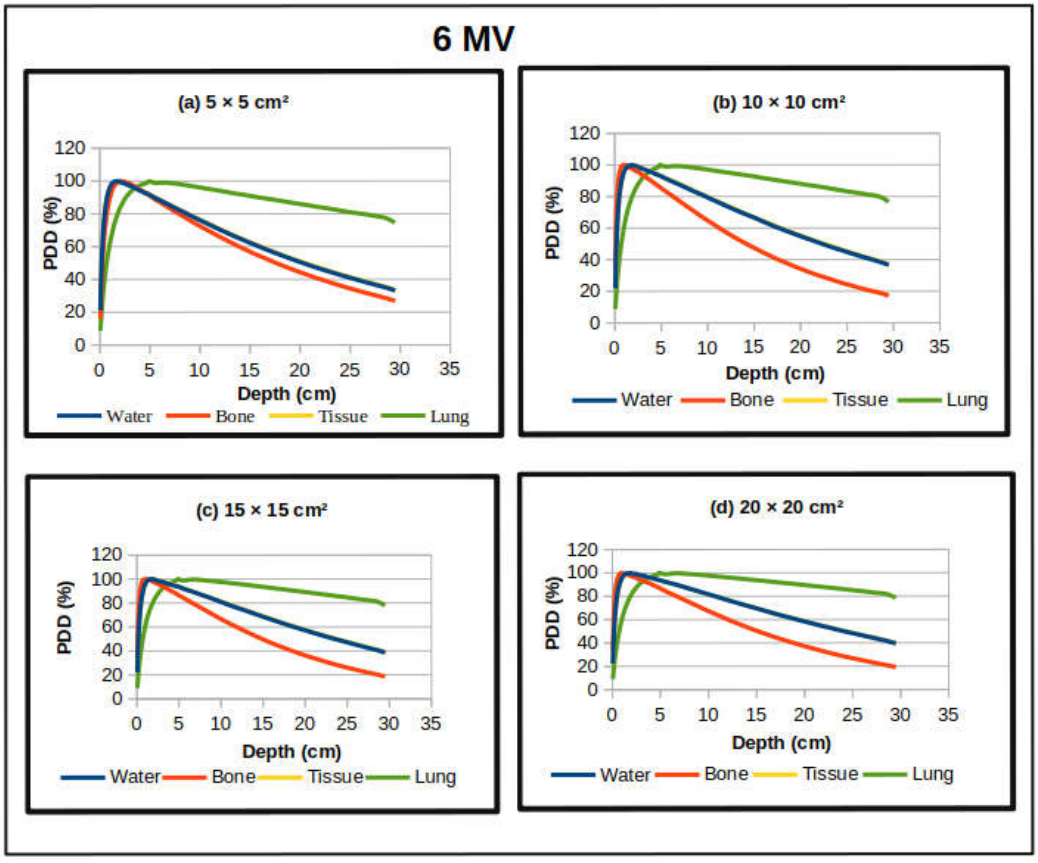

Figure 1: Percentage Depth Dose curves with field sizes of (a) 5×5 cm², (b) 10×10 cm², (c) 15×15 cm², and (d) 20×20 cm² using 6 MV photon energy

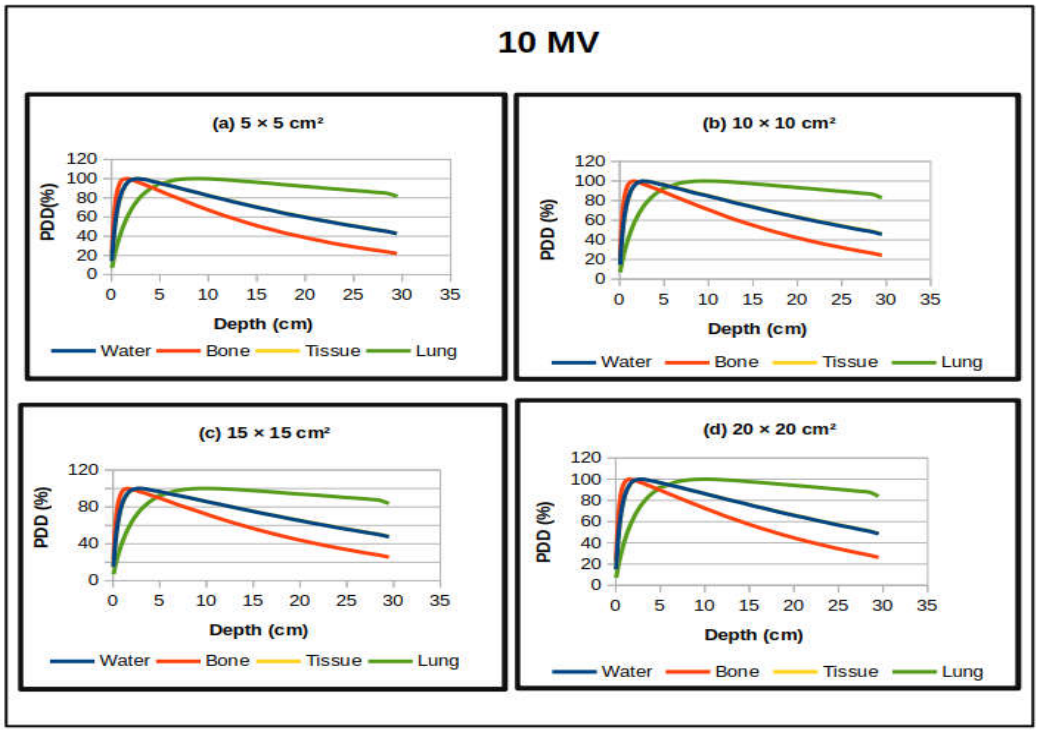

Figure 2: Percentage Depth Dose curves with field sizes of (a) 5×5 cm², (b) 10×10 cm², (c) 15×15 cm², and (d) 20×20 cm² using 10 MV photon energy

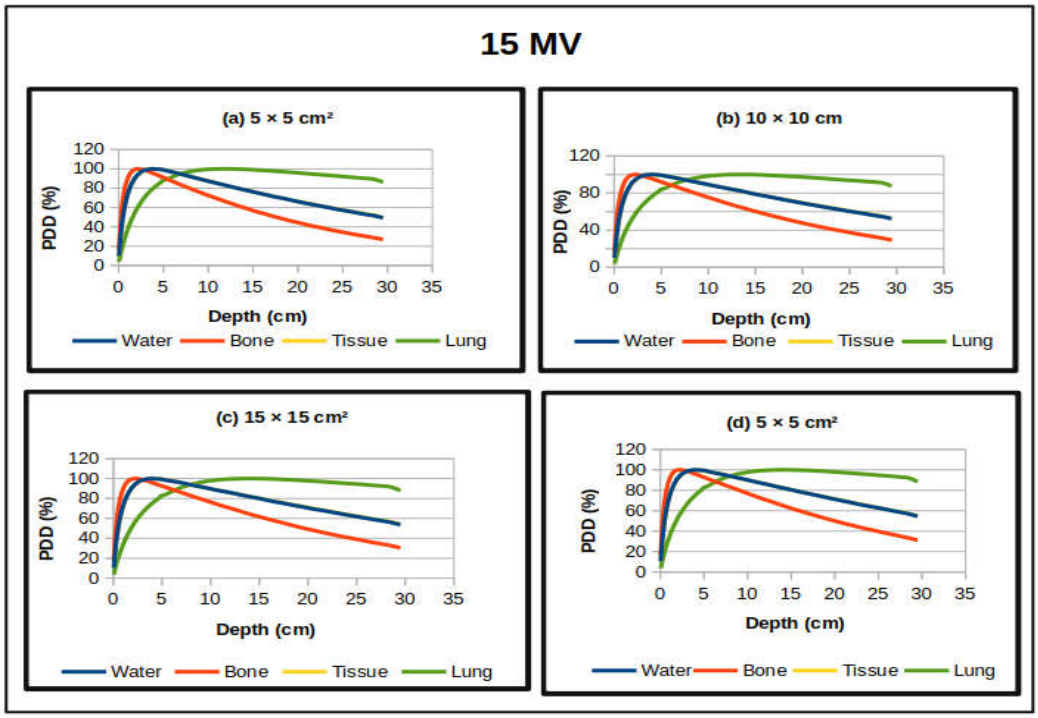

Figure 3: Percentage Depth Dose curves with field sizes of (a) 5×5 cm², (b) 10×10 cm², (c) 15×15 cm², and (d) 20×20 cm² using 15 MV photon energy

6132

Table 2: Comparison of beam flatness and symmetry for different photon energies and media

		6 MV		10 MV		15 MV	
Material	**Field Size (cm x cm)**	**Beam Flatness (%)**	**Beam Symmetry (%)**	**Beam Flatness (%)**	**Beam Symmetry (%)**	**Beam Flatness (%)**	**Beam Symmetry (%)**
Water	5x5	0.406	0.006	0.160	0.241	0.135	0.043
	10x10	0.170	0.014	0.060	0.091	0.125	0.181
	15x15	0.075	0.116	0.065	0.167	0.250	0.031
	20x20	0.305	0.059	0.271	0.120	0.170	0.065
Bone	5x5	0.250	0.120	0.811	0.116	0.185	0.081
	10x10	0.070	0.023	0.060	0.165	0.110	0.152
	15x15	0.205	0.029	0.100	0.060	0.195	0.078
	20x20	0.150	0.059	0.305	0.008	0.145	0.037
Soft Tissue	5x5	0.356	0.081	0.246	0.093	0.497	0.158
	10x10	0.140	0.070	0.210	0.014	0.125	0.002
	15x15	0.085	0.009	0.255	0.412	0.346	0.001
	20x20	0.250	0.014	0.305	0.028	0.105	0.036
Lung	5x5	0.755	0.217	0.346	0.012	0.628	0.156
	10x10	0.245	0.014	0.265	0.073	0.477	0.027
	15x15	0.232	0.046	0.250	0.025	0.095	0.076
	20x20	0.305	0.037	0.381	0.004	0.120	0.066

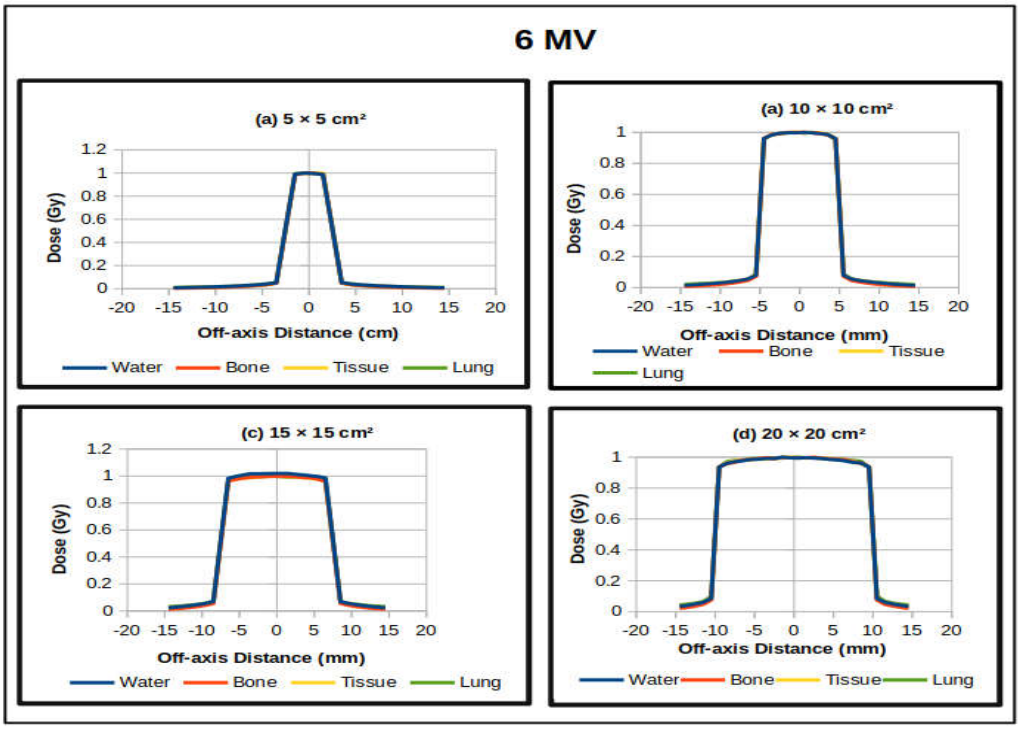

Figure 4: Depth dose profile curves with field sizes of (a) 5×5 cm², (b) 10×10 cm², (c) 15×15 cm², and (d) 20×20 cm² using 6 MV photon energy

6133

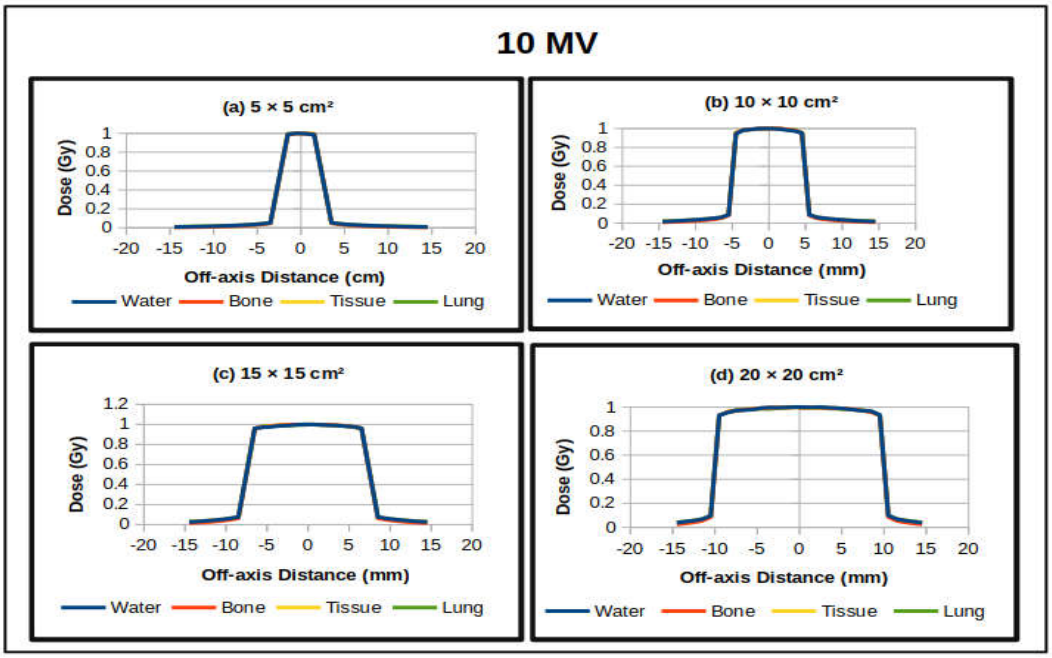

Figure 5: Depth dose profile curves with field sizes of (a) 5×5 cm², (b) 10×10 cm², (c) 15×15 cm², and (d) 20×20 cm² using 10 MV photon energy

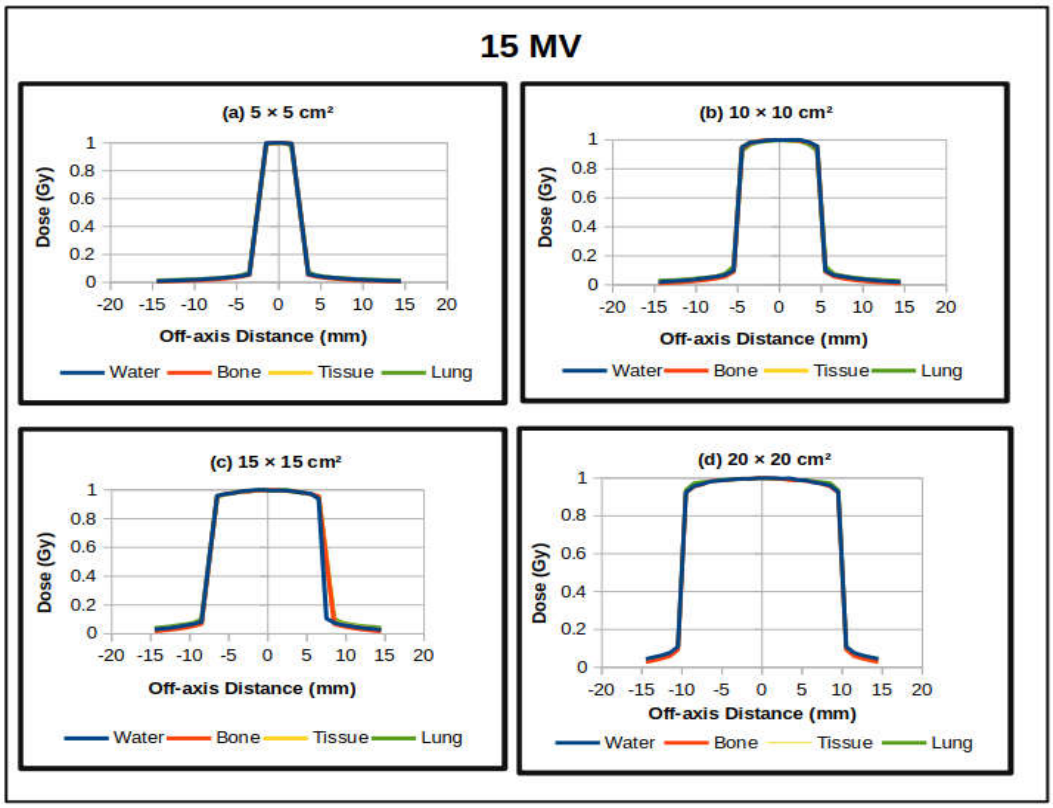

Figure 6: Depth dose profile curves with field sizes of (a) 5×5 cm², (b) 10×10 cm², (c) 15×15 cm², and (d) 20×20 cm² using 15 MV photon energy

4.0 Discusssion

Using the DOSXYZnrc Monte Carlo simulation code, this study assessed photon-beam properties for 6 MV, 10 MV, and 15 MV photon energies in lung, bone, tissue, and water phantoms. Percentage Depth Dose (PDD), lateral dose profiles, and beam uniformity characteristics (flatness and symmetry) were the main subjects of analyses for field sizes ranging from 5×5 cm² to 20×20 cm² at a Source-to-Surface Distance (SSD) of 100 cm. The findings in Table 2 and Figures 1-6 show that photon energy, field size, and material density have a major impact on the features of the dose distribution. The PDD curves (Figures 1-3) showed a significant reliance on tissue type, field size, and photon energy.

According to (Khan & Gibbons, 2014; Podgorsak, 2005), the skin-sparing effect characteristic of megavoltage beams was confirmed by the D_{max} that occurred between 1.7 and 1.9 cm in water at 6 MV with surface doses of 21-22%. Similar depth-dose trends were seen in tissue because it is water-equivalent, but bone, which has a higher density, had a deeper D_{max} (0.9-1.1 cm) and a higher surface dose because of increased backscatter and attenuation (Keall *et al.,* 2006).

In contrast, the lung's lower density resulted in a deeper D_{max} (≈ 4.9 cm) and a lower surface dose. This is in line with (Kita *et al.,* 2023) findings that lower tissue density prevents photon attenuation and postpones the accumulation of maximum dose.

In every medium, D_{max} increased as photon energy increased. D_{max} showed improved photon penetration and decreased surface dose, ranging from 2.5 to 2.9 cm at 10 MV to 2.8 to 3.3 cm at 15 MV (Khan & Gibbons, 2014; Rogers, Walters, & Kawrakow, 2011).

Field size similarly affected the behaviour of PDD. Greater lateral and forward scatter in larger fields (15×15 cm², 20×20 cm²) resulted in somewhat higher doses above D_{max} and broader PDD curves. (Leanderson *et al.,* 2023) discovered a similar relationship in voxel-based Monte Carlo dosimetry, while (Ayata *et al*. (2011) observed that increasing field size in IMRT fields improved scatter equilibrium and dose uniformity. These findings are consistent with this tendency.

Overall, the pattern of increasing D_{max} depth and smoother fall-off with photon energy and field size matches previous experimental observations summarized by (Khan & Gibbons, 2014; Podgorsak, 2005), confirming the reliability of the present simulation setup. The beam homogeneity across various media and field sizes was revealed by the lateral dosage profiles.

Good beam quality was indicated by the flat, symmetric profiles with small penumbrae that were seen in both water and tissue at 6 MV (Podgorsak, 2005). Consistent with the findings of (Yabsantia *et al.,* 2023) on field size, who found that increase lateral scatter with large field size gave a smooth beam profiles.

The lateral gradients in bone were steeper, which is in line with the findings of Keall *et al.,* 2006), who found that electron transport was limited in strong materials. In contrast, the lung displayed wider profiles as a result of lower electron stopping power. This is consistent with (Kita *et al.,*2023) findings that under megavoltage irradiation, low-density lung tissue showed more lateral dose dispersion.

At higher energies (10 MV and 15 MV), beam profiles in water and tissue became progressively flatter and more uniform. Larger fields continued to widen profiles, especially in low-density media, due to increased scatter and extended electron range (Kita *et al.,* 2023; Printzell *et al.,* 2023). This is in line with the findings by (Bencheikh et al., 2017) who found that increasing energy gives a good beam uniformity while widening the lateral spread in heterogeneous media.The results presented in Table 2 showed that all photon beams were within clinical tolerance in line with (Khan & Gibbons 2014: Podgorsak, 2005). All the energies and materials had a flatness within ±3%. Lung had a large divergence of 0.755% for a field size of 5 × 5 cm^2, which was a result of scatter equilibrium in a low-density region. Restricting the lateral photon results in the rise in off-axis variation in small fields as found by (Ayata *et al.*, 2011).

In water and tissue, flatness was uniform with a little increase as field size was increased, showing better scatter correction. Beam symmetry was within ±2%. Asymmetry in the lung was caused by low density and reduced backscatter,

supporting the studies by (Pascal *et al.,* 2022) and (Andreo *et al.,* 2018), which highlighted the ability of DOXYZnrc to reproduce beam symmetry in heterogenous media accurately.

The beam flatness across all the materials ranged from 0.060% to 0.811%. Large variation was seen in a small field of 5 × 5 cm^2 of low-density lung medium reaching 0.755%, while beam symmetry ranged from 0.001% to 0.241%. From the findings, there are important practical implications in the radiotherapy treatment plan. The shift in D_{max} and increased flatness in lung tissue, particularly in small fields, calls for careful dose modeling in thoracic treatment such as stereotactic body radiotherapy, where small fields are commonly used.

Study Limitations

A simplified geometry and source were used for this study, which didn't capture complex patient anatomy. Future work will focus on analyzing complex phantoms or clinical treatment.

5.0 Conclusion

This study utilized DOSXYZnrc Monte Carlo code to assess how photon beams of 6 MV, 10 MV, and 15 MV behave in water, lung, tissue, and bone. Dose distributions were affected by field size and photon energy, of which large field sizes improve dose uniformity and scatter equilibrium and high energy enables skin-sparing effects and beam penetration. The simulated beams stayed within clinical tolerance and symmetry at ±3% and ±2%, which makes DOSXYZnrc a reliable and essential tool for understanding beam characteristics and for verifying dose calculations in heterogenous media, thereby supporting more accurate radiotherapy treatment plans.

Conflict of Interest

None

References

Andreo, P. (2018). Monte Carlo simulations in radiotherapy dosimetry. *Radiation Oncology Journal,* 36(1): 1–11.

Ayata, H. B., Güden, M., Ceylan, C., Kücük, N., and Engin, K. (2011). Comparison of dose distributions and organs at risk (OAR) doses in conventional tangential technique (CTT) and IMRT plans with different numbers of beams in left-sided breast cancer. *Reports of Practical Oncology and Radiotherapy,* 16(3): 95–102.

Baumann, M., Krause, M., Overgaard, J., Debus, J., Bentzen, S. M., Daartz, J., Richter, C., Zips, D., and Bortfeld, T. (2016). Radiation oncology in the era of precision medicine. *Nature Reviews Cancer,* 16(4): 234–249.

Bencheikh, M., Maghnouj, A., Tajmouati, J., Didi, A., and Ezzati, A. O. (2017). Validation of Monte Carlo simulation of 6 MV photon beam produced by Varian Clinac 2100 linear accelerator using BEAMnrc code and DOSXYZnrc code. *Physics of Particles and Nuclei Letters,* 14(5): 780–787.

Followill, D. S., Davis, D. S., and Ibbott, G.S. (2004). Comparison of electron beam characteristics from multiple accelerators. *International Journal of Radiation Oncology, Biology, Physics,* 59(3): 905–910.

Keall, P. J., Siebers, J. V., Jeraj, R., and Mohan, R. (2006). Radiotherapy dose calculations in the presence of high-density materials. *Physics in Medicine and Biology,* 51(5): 893–907.

Khan, F. M., and Gibbons, J. P. (2014). *The physics of radiation therapy.* 5th ed. Lippincott Williams & Wilkins.

Kito, M., Tsukahara, Y., Okamoto, M., Yoshimura, K., and Kataoka, M. (2023). Does re-ossification after palliative radiotherapy for spinal bone metastases help maintain vertebral body height? *The Spine Journal,* 23(10): 1540–1548.

Kita, N., Yamazaki, H., Nakamura, S., Tachi, K., Suzuki, G., and Yamada, K. (2023).

Clinical and dosimetric factors for symptomatic radiation pneumonitis after stereotactic body radiotherapy for early-stage non-small cell lung cancer. *Clinical and Translational Radiation Oncology,* 41: 100661.

Leanderson, P. C. C., de Sá, L.V., Kitamikado, R. A., Sapienza, M. T., and Bonifácio, D. A. B. (2023). Optimized Monte Carlo simulations for voxel-based internal dosimetry. *Physics in Medicine and Biology,* 68(11): 115003

Machichi, M., Oulhouq, Y., Rrhioua, A., Zerfaoui, M., and Bakari, D. (2019). Simulation of the dose calculation and distribution in Radiation Therapy Treatment Planning System. *Materials Today Proceedings,* 13: 982–990.

Paschal, H. M., Kabat, C. N., Papaconstadopoulos, P., Kirby, N.A., Myers, P. A., Wagner, T. D., and Stathakis, S. (2022). Monte Carlo modeling of the Elekta Versa HD and patient dose calculation with EGSnrc/BEAMnrc. *Journal of Applied Clinical Medical Physics,* 23(9): e13704.

Podgorsak, E. B. (2005). *Radiation oncology physics: A handbook for teachers and students.* International Atomic Energy Agency.

Printzell, L., Reseland, J. E., Edin, N. F. J., Tiainen, H., and Ellingsen, J. E. (2023). The dose-dependent impact of γ-radiation reinforced with backscatter from titanium on primary human osteoblasts. *Biomaterials Investigations in Dentistry,* 10(1): 2209116.

Rogers, D. W. O., Walters, B. R. B., and Kawrakow, I. (2011). *BEAMnrc users manual.* National Research Council of Canada.

Sladowska, A., Hojreh, A., Georg, D., and Fuchs, H. (2011). Risks and uncertainties in advanced IMRT: Lessons from clinical practice. *Strahlentherapie und Onkologie,* 187(6): 367–373.

Yabsantia, S., Suriyapee, S., Phaisangittisakul, N., Oonsiri, S., Sanghangthum, T., and Seuntjens, J. (2023). Investigation of field output factors using IAEA-AAPM TRS-483 code of practice recommendations and Monte Carlo simulation for 6 MV photon beams. *Journal of Radiotherapy in Practice,* 22(2): 174–179.